

# Formation of pentagonal atomic chains in BCC Fe nanowires

G. Sainath<sup>1, a)</sup> and B.K. Choudhary<sup>1, b)</sup>

*Deformation and Damage Modelling Section, Metallurgy and Materials Group,  
Indira Gandhi Center for Atomic Research, HBNI, Kalpakkam, Tamilnadu -603102,  
India*

For the first time, we report the formation of pentagonal atomic chains during tensile deformation of ultra thin BCC Fe nanowires. Extensive molecular dynamics simulations have been performed on  $\langle 100 \rangle / \{110\}$  BCC Fe nanowires with different cross section width varying from 0.404 to 3.634 nm at temperatures ranging from 10 to 900 K. The results indicate that above certain temperature, long and stable pentagonal atomic chains form in BCC Fe nanowires with cross section width less than 2.83 nm. The temperature, above which the pentagonal chains form, increases with increase in nanowire size. The pentagonal chains have been observed to be highly stable over large plastic strains and contribute to high ductility in Fe nanowires.

**Keywords:** Molecular dynamics simulations, BCC Fe Nanowire, Plastic deformation, Pentagonal atomic chains

## I. INTRODUCTION

In recent years, metallic nanowires have attracted a major attention for research due to their unique properties and potential applications in future nano/micro electro-mechanical systems. The nanowires suspended between two electrodes are found to exhibit the electron transport properties similar to that of a quantum wire which shows a quantized conductance, and it has gained importance in fundamental physics and in electronic device technology as a quantized conductance atomic switch<sup>1</sup>. Under tensile loading, if the cross-section area of nanowire reduces to that of a few-atom thickness prior to failure, it exhibits conductance in multiples of  $G_0 = 2e^2/h$ , where  $e$  is the electron charge and  $h$  is the Plancks constant<sup>2</sup>. In view of this correlation between the structure and the conductance, it is important to understand the formation and the stability of the long atomic chains during deformation of metallic nanowires. Further, the 1-D structures can also act as ideal systems to understand the low-dimensional physics.

In the past, the formation of the linear, pentagonal and other multi-shell atomic chains have been observed during the deformation of many FCC nanowires and the formation of all these atomic chains is associated with the quantized conductance<sup>2-7</sup>. The long linear atomic chains have been observed experimentally during the stretching of Au and Cu nanowires<sup>2-4</sup>. The linear atomic chains display conductance close to  $G_0$ . Using transmission electron microscopy, Gonzalez et al.<sup>5</sup> observed the formation of pentagonal chains during the stretching of Cu nanowires which exhibited the conductance of  $4.5G_0$ . During tension deformation, the Au nanowires have been found to exhibit a zigzag shape, which remains stable even if the load is relieved<sup>6</sup>. Similarly, Kondo and Takayanagi<sup>7</sup> synthesized the gold nanowires with diame-

ter as small as 0.6 nm having length of 6 nm. Using high-resolution electron microscopy, it has been found that these nanowires have a multi-shell structure composed of coaxial tubes<sup>7</sup>. Each tube consists of helical atom rows coiled round the wire axis. The structures such as linear atomic chain (monatomic, diatomic), pentagonal, two-shell, three-shell and helical multi-shell structures have also been predicted theoretically in ultra thin Al and Pb metallic nanowires<sup>8</sup> and also in ZnO and Si semiconductor nanowires using molecular dynamics simulations<sup>9,10</sup>. In Al and Pb metallic nanowires, it has been postulated that the competition between optimal internal packing and minimal surface energy is the main driving force behind these morphological structures at small size<sup>8</sup>. However, out of all these structures, the formation of pentagonal atomic chains is one of the fascinating observations as it exhibits a five-fold symmetry with respect to the nanowire axis and does not correspond to any of the 14 Bravais lattices. Generally, the pentagonal structure is not observed in 2-D or 3-D structures as it is incompatible with the translational symmetry. However, as mentioned above, the strong evidence of pentagonal structures have been found experimentally in 1-D structures, such as ultra-thin Cu nanowires<sup>5</sup>. In agreement with experimental observations, many atomistic simulation studies have also shown the formation of pentagonal atomic chains in Cu<sup>11-13</sup>, Al<sup>13</sup>, Ni<sup>13,14</sup>, and Au<sup>15,16</sup>. The pentagonal structures have also been observed in HCP Mg nanowires during the atomistic simulations studies<sup>17,18</sup>. The evidence of pentagonal structures has been found during the stretching of BCC Na nanowires using first-principles molecular dynamics simulations<sup>19</sup>[19]. Other than Na, the pentagonal structure has not been reported in any other metallic BCC nanowires either by experiments or atomistic simulations. For the first time in this paper, we report the formation of long pentagonal atomic chains in ultra thin BCC Fe using molecular dynamics (MD) simulations. Further, the formation mechanism and the range of nanowire size and temperatures over which pentagonal atomic chains form are presented.

<sup>a)</sup> Electronic mail: [sg@igcar.gov.in](mailto:sg@igcar.gov.in)

<sup>b)</sup> Electronic mail: [bkc@igcar.gov.in](mailto:bkc@igcar.gov.in)

## II. MOLECULAR DYNAMICS SIMULATIONS

Molecular dynamics (MD) simulations have been performed using LAMMPS package<sup>20</sup> employing an embedded atom method (EAM) potential for BCC Fe given by Mendelev and co-workers<sup>21</sup>. BCC Fe nanowires oriented in  $\langle 100 \rangle$  axial direction with  $\{110\}$  as side surfaces were considered in this study. Simulations have been performed on nanowires with cross section width ( $d$ ) ranging from 0.404 to 3.634 nm. In all nanowires, the length ( $l$ ) was twice the cross section width. Periodic boundary conditions were chosen along the nanowire length direction, while the other directions were kept free in order to mimic an infinitely long nanowire. After the initial construction of nanowire, energy minimization was performed by conjugate gradient method to obtain a stable structure. Velocity verlet algorithm was used to integrate the equations of motion with a time step of 5 femto seconds. Finally, the model system was thermally equilibrated to a required temperature in canonical ensemble with a Nose-Hoover thermostat. For each nanowire cross section width, the simulations have been performed at different temperatures ranging from 10 to 900 K. Following thermal equilibration, the tensile deformation was performed at a constant strain rate of  $1 \times 10^8 \text{ s}^{-1}$  along the axis of the nanowire. The strain rate considered during deformation is significantly higher than the typical experimental strain rates. This is due to the inherent timescale limitations from MD simulations. Here, it must be noted that the strain rate also influences the formation of linear and pentagonal atomic chains<sup>9,12</sup>. For each size and temperature, five independent simulations have been carried out to make statistically meaningful conclusions. The average stress was calculated from the Virial expression<sup>22</sup>. The visualization of atomic configurations was performed using AtomEye package<sup>23</sup> with coordination number and common neighbour analysis (CNA). In solid-state systems, the CNA pattern is useful for obtaining local crystal structure around an atom<sup>24,25</sup>. In the present analysis, this method is used to distinguish the atoms in crystalline, non-crystalline and pentagonal or icosahedral environment.

## III. RESULTS AND DISCUSSION

Molecular dynamics simulations have been carried out on BCC Fe nanowires with cross section width varying from 0.404 to 3.634 nm at different temperatures ranging from 10-900 K. The atomic snapshots demonstrating the formation of pentagonal atomic chains before failure during tensile deformation of BCC Fe nanowire are typically shown for  $d = 1.615 \text{ nm}$  at 600 K in Fig. 1. Initially, the nanowire undergoes yielding followed by an extensive plastic deformation dominated by the slip of  $1/2[111]$  full dislocations (Fig. 1a). With increasing strain, the plastic deformation occurs on multiple slip systems and leads to necking with disordered or non-

crystalline atomic structure shown in Fig. 1(b). When the cross section of the neck region is close to a few atomic spacings, some of the disordered atoms rearrange themselves and forms pentagonal unit cell shown in Fig. 1(c). Following this, the five atom rings are added successively to the structure unit by unit at the expense of disordered atoms in the necking region and this leads to increase in the length of pentagonal atomic chain (Fig. 1d). This continuous process occurs until failure resulting in the formation of long pentagonal atomic chain in the necking region (Figs. 1(e-f)). The maximum attained length of the pentagonal atomic chain has been obtained to be 3.2 nm consisting of 13 pentagonal rings. The formation of long pentagonal chains indicates the stability at high strains and this contributes to large plastic deformation and high ductility in small size BCC Fe nanowires. In order to obtain detailed understanding of structural aspects of pentagonal atomic chain, a single unit cell of the long chain is presented in Fig. 1(g). It can be seen that the pentagonal chain consists of a central atom having a coordination of 10 atoms enclosed by two pentagonal rings  $L_1$  and  $L_2$ . The long atomic chain has 1-5-1-5 stacking sequence with successive pentagonal rings  $L_1$  and  $L_2$  rotated by  $\pi/5$  (Fig. 1h). This structure is known as staggered pentagon and has 12 atoms in each unit cell. The stability of staggered pentagonal structure in Fe is confirmed by Sen et al.<sup>26</sup> using first principle calculations. The relevant inter atomic distances and the bond angles in the pentagonal unit cells for small size ( $d = 0.807 \text{ nm}$ ) and large size ( $d = 1.615 \text{ nm}$ ) Fe nanowire at 600 K are listed in Table I. A good agreement between the inter-atomic distances and bond angles obtained in the present study and those calculated by Sen et al.<sup>26</sup> for free pentagonal nanowires using first principle calculations can be clearly seen in Table I.

The formation of pentagonal atomic chains as a function of the combination of nanowire size and temperature is shown in Fig. 2. It can be clearly seen that the formation of pentagonal atomic chains is promoted by decrease in nanowire size and increase in temperature. The range of nanowire size over which pentagonal atomic chains are formed increases with increase in temperature. In fact, for each nanowire size, a transition temperature exists above which the pentagonal atomic chains are formed. The transition temperature increases linearly with increase in nanowire size. It is important to point out that the pentagonal atomic chains are not formed at low temperatures of 10 and 100 K as well as nanowire size larger than 2.83 nm. The observed formation of pentagonal atomic chains promoted by small nanowire size and higher temperatures is in agreement with those reported for FCC and HCP nanowires<sup>11-18</sup>. In addition to above, it has been shown that the crystallographic orientation and strain rate influence the formation of pentagonal atomic chains during tensile deformation in FCC nanowires<sup>12-14</sup>. The combined effect of temperature and strain rate on the formation of linear atomic chains in ZnO nanowires has been explained

TABLE I. Comparison of inter-atomic distances and the bond angles in pentagonal unit cells for small ( $d = 0.807$  nm) and large ( $d = 1.615$  nm) size nanowires at 600 K with those reported based on first principles calculations.  $d_{ij}$  indicates the distance between the atoms  $i$  and  $j$  in Figure 1(g) and  $\angle ijk$  indicates the bond angle between the  $i, j$  and  $k$  atoms.

	$d_{12}$	$d_{13}$	$d_{34}$	$d_{46}$	$\angle 314$	$\angle 315$	$\angle 316$	$\angle 317$	$\angle 364$
Small ( $d = 0.87$ nm)	2.40	2.50	2.62	2.72	62.17	110.38	65.52	111.62	57.29
Large size ( $d = 1.42$ nm)	2.37	2.56	2.75	2.74	65.15	116.4	66.16	119.8	58.74
First principles calculations <sup>26</sup>	2.16	2.31	2.39	2.51	62.4	114.2	65.8	117.5	57.00

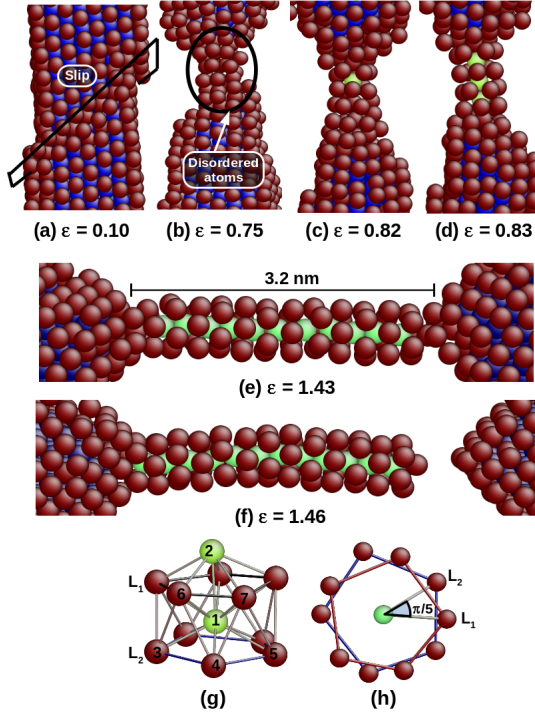


FIG. 1. The formation of pentagonal atomic chain in the necking region of BCC Fe nanowire with  $d = 1.615$  nm during tensile deformation at 600 K. The atoms are coloured according to CNA. The blue colour indicates the atoms in BCC structure, the red colour indicates the atoms in disordered structure including surfaces and light green colour indicates the atoms in pentagonal or icosahedral symmetry.

based on the Arrhenius model<sup>9</sup>. Further, the observation of transition temperature as a function of size in BCC Fe nanowires appears to be significant, since there is no such transition temperature established yet in either FCC<sup>11–16</sup> or HCP nanowires<sup>17,18</sup>. These results indicate that at proper size and temperature, the BCC Fe nanowires can also exhibit long pentagonal atomic chains during the deformation.

The pentagonal atomic chains are observed for the wide range of nanowire sizes and temperatures as shown in Fig. 2. However, there has been significant difference between the pentagonal chains formed in the small and comparatively large size nanowires. In large size nanowires, the formation of pentagonal atomic chains

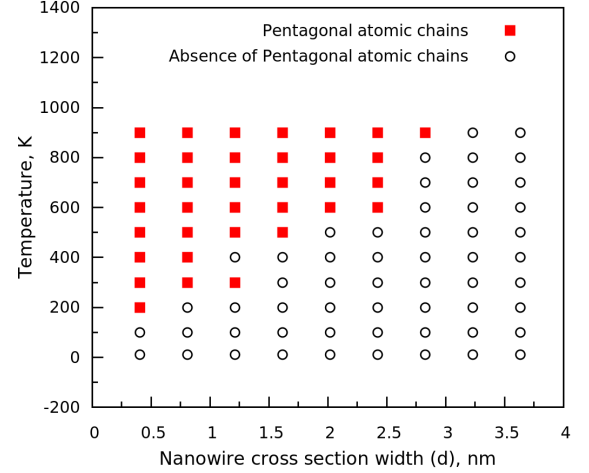


FIG. 2. Temperature vs. nanowire size plot showing the regions of size and temperature over which pentagonal atomic chains (PAC) are formed.

remains limited to necking regions only as observed for nanowire width,  $d = 1.615$  nm in Fig. 1. In case of small size nanowires with  $d = 0.404$  and  $0.807$  nm, complete transformation of full nanowire into pentagonal atomic chains is observed at relatively higher temperatures. This is typically shown for nanowire width  $d = 0.807$  nm at 600 K in Figs. 3(a-e). The progressive plastic deformation resulting in the complete transformation into non-crystalline state and the nucleation of pentagonal atomic chains can be seen in Figs. 3(b) and 3(c), respectively. The complete transformation of full nanowire into pentagonal atomic chains and failure at large strain are presented in Figs. 3(d) and 3(e), respectively. In small size nanowires, the process of pentagonal structure formation remains same as that of the large nanowires. However, the plastic deformation in small size nanowires transforms the complete nanowire into a non-crystalline state (Figs. 3(a-b)), unlike only the neck area in large size nanowires. The complete transformation into pentagonal atomic chains has been observed in nanowires with cross-section width  $d = 0.404$  and  $0.807$  nm at temperatures above 400 and 500 K, respectively (Fig. 2). The transformation into non-crystalline structure (Fig. 3b) can be understood in terms of internal atomic rearrangements to maximize the overall atomic coordination leading to an increase in cohesive energy<sup>13</sup>. Following

the disordered state, the pentagonal unit cell nucleates out of this to minimize the surface energy (Fig. 3c) and grows all along the nanowire leading to long and stable pentagonal nanowire (Fig. 3d). In small size nanowires ( $d = 0.807$  nm), the long pentagonal atomic chains consisted of as many as 25 pentagonal rings compared to 13 rings in large size nanowire with  $d = 1.615$  nm at 600 K. The observed long pentagonal atomic chains remain stable during the deformation and contribute to large failure strains as much as 265% in small size nanowires.

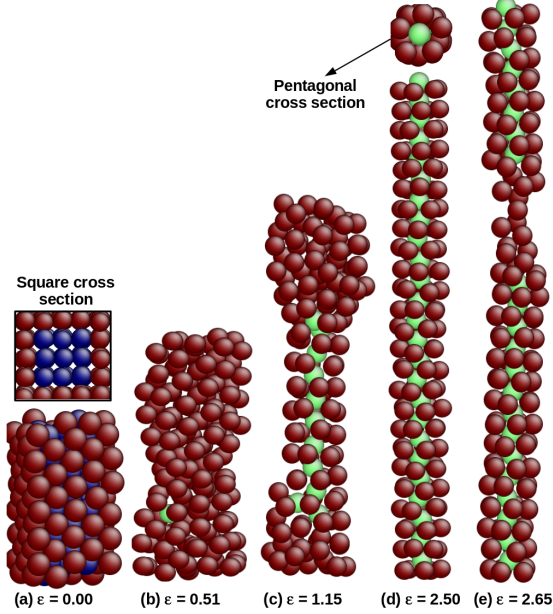


FIG. 3. The complete transformation of BCC Fe nanowire with  $d = 0.807$  nm into long pentagonal nanowire at 600 K. (a) Initial BCC structure, (b) the disordered structure along with nucleation of pentagonal atomic chain, (c) growth of pentagonal atomic chain (d) completely transformed into pentagonal atomic chains and (e) onset of necking and failure. The atoms are coloured according to CNA. The blue colour indicates the atoms in BCC structure, the red colour indicates the atoms in disordered structure including surfaces and light green colour indicates the atoms in pentagonal or icosahedral symmetry.

Typical stress-strain behaviour of BCC Fe nanowires exhibiting the formation of pentagonal chain at 600 K and in absence of pentagonal chain at 10 K is shown in Fig. 4 for nanowire with  $d = 1.615$  nm. In case of nanowire showing the formation of pentagonal atomic chains, large flow stress oscillations in terms of sharp peaks and drops due to continuous plastic deformation by dislocation slip can be seen up a strain of 0.77. Here, each flow stress peak and drop corresponds to dislocation nucleation, propagation and annihilation. Once neck forms in the nanowire, the nucleation of pentagonal atomic structure and its growth along the nanowire axis leads to constant plateau as observed in the strain range 0.77-1.47. In general, the formation of pentagonal atomic chains facilitates high ductility in BCC Fe nanowires. On the other hand, the nanowires that do

not show the formation of pentagonal structures exhibit different stress-strain behaviour in terms of flow stress oscillations and the second elastic peak. Unlike deformation by slip in nanowires showing pentagonal chains, the plastic deformation by twinning leading to complete reorientation from initial  $\langle 100 \rangle / \{110\}$  to  $\langle 110 \rangle / \{100\}$  orientation has been observed in nanowires that do not show the formation of pentagonal structures. The large second peak in stress-strain behaviour at 10 K is due to the elastic deformation of the reoriented nanowire. With increasing strain, this reoriented nanowire undergoes deformation by slip, but this has not lead to diffused necking and as a result, the pentagonal atomic chains were not observed. Detailed studies on  $\langle 100 \rangle$  BCC Fe nanowires have shown that the deformation by twinning followed by reorientation occurs at 10 K<sup>27-29</sup>. This result shows that the orientation nanowire also influence the formation of pentagonal atomic chains in BCC Fe nanowires.

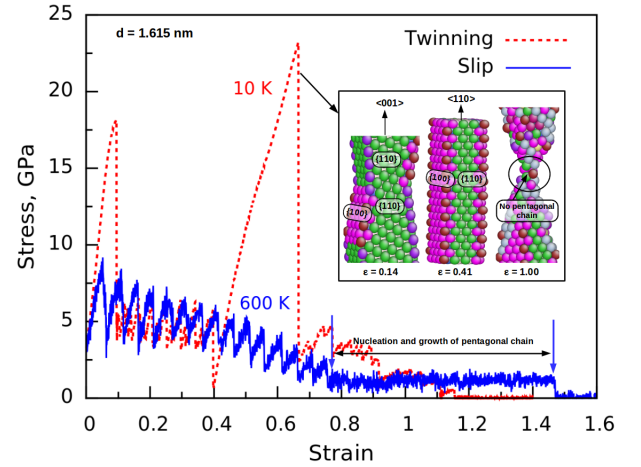


FIG. 4. Typical stress-strain behaviour exhibiting occurrence of pentagonal chains at 600 K and its absence at 10 K for BCC Fe nanowires with  $d = 1.615$  nm are shown by full and broken lines respectively. The nucleation and growth of pentagonal atomic chains at 600 K are marked in the Figure. The nanowires which do not exhibit pentagonal structure and deform by twinning followed by reorientation are shown in the inset at 10 K.

#### IV. CONCLUSIONS

We have performed extensive molecular dynamics simulations on the tensile deformation of ultra thin BCC Fe nanowires. The results indicated that long pentagonal atomic chains are formed in the diffused necking region of small size  $\langle 100 \rangle / \{110\}$  BCC Fe nanowires. The complete transformation to the pentagonal structures has been observed in nanowires with  $d = 0.404$  and  $0.807$  nm at higher temperatures. The temperature above which the pentagonal atomic chains are formed increases with increase in the size of nanowire, and above a critical size of  $2.83$  nm, the pentagonal atomic



chains are not observed at any temperature. BCC Fe nanowires exhibiting pentagonal structure undergo deformation by slip mechanism. The nanowires which do not exhibit pentagonal structure deform by deformation twinning mechanism and undergo reorientation from the initial  $\langle 100 \rangle / \{110\}$  orientation to  $\langle 110 \rangle / \{100\} \{110\}$  orientation.

- <sup>1</sup>K. Terabe, T. Hasegawa, T. Nakayama, M. Aono, *Nature*, 433 (2005) 47-50.
- <sup>2</sup>H. Ohnishi, Y. Kondo, K. Takayanagi, *Nature* 395 (1998) 780-783.
- <sup>3</sup>P.Z. Coura, S.B. Legoas, A.S. Moreira, F.Sato, V. Rodrigues, S.O. Dantas, D. Ugarte, D.S. Galvao, *Nano Lett.*, 4 (2004) 1187-1191.
- <sup>4</sup>F. Sato, A.S. Moreira, J. Bettini, P.Z. Coura, S.O. Dantas, D. Ugarte, D.S. Galvao, *Phys. Rev. B* 74 (2006) 193401.
- <sup>5</sup>J. C. Gonzalez, V. Rodrigues, J. Bettini, L.G.C. Rego, A.R. Rocha, P.Z. Coura, S.O. Dantas, F. Sato, D.S. Galvao, D. Ugarte, *Phys. Rev. Lett.* 93 (2004) 126103.
- <sup>6</sup>D. Sanchez-Portal, E. Artacho, J. Junquera, P. Ordejon, A. Garcia, J.M. Soler, *Phys. Rev. Lett.* 83 (1999) 3884-87.
- <sup>7</sup>Y. Kondo, K. Takayanagi, *Science*, 289 (2000) 606-608.
- <sup>8</sup>O. Gulseren, F. Ercolessi, E. Tosatti, *Phys. Rev. Lett.* 80 (1998) 3775-78.
- <sup>9</sup>B.B. Wang, F.C. Wang, Y.P. Zhao, *Science China Phys. Mech. Astro.* 55 (2012) 1138-1146.
- <sup>10</sup>F.C. Wang and Y.P. Zhao, *Arch. Appl. Mech.* 85 (2015) 323-329.
- <sup>11</sup>V.K. Sutrakar, D.R. Mahapatra, *J. Phys.: Condens. Matter* 20 (2008) 335206.
- <sup>12</sup>V.K. Sutrakar, D.R. Mahapatra, *Nanotech.* 20 (2009) 045701.
- <sup>13</sup>P. Garcia-Mochales, S. Pelaez, P.A. Serena, C. Guerrero, R. Paredes, *Modelling Simul. Mater. Sci. Eng.* 21 (2013) 045002.
- <sup>14</sup>P. Garcia-Mochales, R. Paredes, S. Pelaez, P.A. Serena, *Phys. Stat. Sol.* 205 (2008) 1317-1323.
- <sup>15</sup>H.S. Park, J.A. Zimmerman, *Phys. Rev. B* 72 (2005) 054106.
- <sup>16</sup>H.S. Park, J.A. Zimmerman, *Scr. Mater.* 54 (2006) 1127-1132.
- <sup>17</sup>A. Takahashi, S. Kurokawa, A. Sakai, *Phys. Stat. Sol. B*, 251 (2014) 1363-1371.
- <sup>18</sup>N. Fujita, S. Kurokawa, A. Sakai, *Phys. Stat. Sol. B*, 1-7 (2016), DoI:10.1002/pssb.201552544.
- <sup>19</sup>R.N. Barnett, U. Landman, *Nature* 387 (1997) 788-91.
- <sup>20</sup>S.J. Plimpton, *J. Comput. Phys.* 117 (1995) 1-19.
- <sup>21</sup>M.I. Mendeleev, S. Han, D.J. Srolovitz, G.J. Ackland, D.Y. Sun, M. Asta, *Philos.Mag.* 83 (2003) 3977-3994.
- <sup>22</sup>J.A. Zimmerman, E.B. Webb, J.J. Hoyt, R.E. Jones, P.A. Klein, D.J. Bammann, *Modelling Simul. Mater. Sci. Eng.* 12 (2003) S319-S332.
- <sup>23</sup>J. Li, *Modelling Simul. Mater. Sci. Eng.* 11 (2003) 173-177.
- <sup>24</sup>D. Faken, H. Jonsson, *Comp. Mater. Sci.* 2 (1994) 279-286.
- <sup>25</sup>H. Tsuzuki, P.S. Branicio, J.P. Rino, *Comp. Phys. Comm.* 177 (2007) 518-523.
- <sup>26</sup>P. Sen, O. Gulseren, T. Yildirim, I.P. Batra, S. Ciraci, *Phys. Rev. B*, 65 (2002) 235433.
- <sup>27</sup>G. Sainath, B.K. Choudhary and T. Jayakumar, *Comp. Mater. Sci.* 104 (2015) 76-83.
- <sup>28</sup>G. Sainath and B.k. Choudhary, *Comp. Mater. Sci.* 111 (2016) 406-415.
- <sup>29</sup>G. Sainath and B.K. Choudhary, *Phil. Mag. Lett.* 96 (2016) 469-76.